

# S-allyl cysteine protects retinal pigment epithelium cells from hydroquinone-induced apoptosis through mitigating cellular response to oxidative stress

Z.-W. SUN, C. CHEN, L. WANG, Y.-D. LI, Z.-L. HU

Department of Ophthalmology, Fourth Affiliated Hospital of Kunming Medical University (the Second People's Hospital of Yunnan Province); Yunnan Eye Institute; The Ocular Disease and Clinical Medicine Research Center of Yunnan Province; The Ocular Disease Clinical Medicine Center of Yunnan Province, Kunming, China

**Abstract.** – **OBJECTIVE:** Retinal pigment epithelium (RPE) degenerative death is an evident hallmark of advanced age-related macular degeneration (AMD). The present study aims to evaluate the protective effects of S-allyl L-cysteine (SAC), a bioactive component from aged garlic extracts, on the oxidative stress-related apoptosis of RPE cells and to investigate the potential underlying mechanisms.

**MATERIALS AND METHODS:** Cell Counting Kit-8 (CCK-8) assay, flow cytometry, and terminal deoxynucleotidyl transferase-mediated dUTP-biotin nick end labeling (TUNEL) staining were performed to evaluate the effects of SAC on the hydroquinone-treated human ARPE19 cells. The Reactive Oxygen Species (ROS) production was measured by virtue of flow cytometry or determined under an inverted fluorescence microscope. Furthermore, the expression of antioxidant factor Nrf2, as well as downstream antioxidant genes, including NQO1, SOD1, SOD2, and HO1 was assessed in hydroquinone stimulated ARPE19 cells, in the presence or absence of SAC pretreatment.

**RESULTS:** Hydroquinone incitement contributed to a marked decrease in cell viability, but enhanced cell apoptosis, whereas SAC addition did not cause significant alterations. When cells were pre-treated with SAC, cell proliferation was dramatically enhanced whereas apoptosis was mitigated, and the ROS generation induced by hydroquinone was also significantly suppressed, indicating a prominent function of SAC in preventing ARPE19 cells from oxidant-related apoptosis. The elevated expression levels of Nrf2 and other antioxidant genes driven by hydroquinone were downregulated by SAC addition.

**CONCLUSIONS:** These data suggest that SAC can effectively attenuate hydroquinone-induced oxidative damage in human RPE cells. Our work

is the first to demonstrate that SAC modulates oxidative stress-induced RPE apoptosis, thereby potentially proving new insights into the treatment of AMD.

*Key Words:*

Age-related macular degeneration, Retinal pigment epithelium, Apoptosis, S-allyl cysteine, Oxidative stress.

## Introduction

Age-related macular degeneration (AMD) is an acquired disease of the macula that represents the predominant cause of central visual loss among the population over 50 years old in developed countries<sup>1</sup>. During recent decades, the morbidity of AMD has been dramatically increased worldwide as a result of the rapidly growing aging population<sup>2</sup>. AMD can be clinically classified into either dry or wet form, with the former comprising ~85% of all diagnosed cases. Retinal pigment epithelium (RPE) is a single layer of non-dividing cells which play a crucial role in the maintenance of neuroretinal hemostasis and photoreceptor cell survival. RPE cell death caused by oxidative stress, mostly attributed to apoptosis, as well as necrosis, is significantly implicated in AMD pathogenesis<sup>3-5</sup>. Furthermore, during the process of aging RPE undergoes an array of pathological changes that will cause deposits of lipofuscin within the macula, which is known as drusen. Individuals presented with drusen and other ocular disturbances usually have an increased risk of progressing into advanced dry AMD or even vision loss<sup>6</sup>.

Although the etiology of AMD is complicated and heterogeneous, there are multiple established risk factors which are responsible for this disease, including aging, gene polymorphisms, as well as several environmental factors such as cigarette smoking, dietary habits, and phototoxic exposure<sup>7</sup>. Among them, active or passive smoking has been considered as an independent risk factor for the initiation and/or development of AMD<sup>8,9</sup>. Using experimental animal models, Fujihara et al<sup>10</sup> found that the exposure to smoke for a long term leads to RPE apoptosis and oxidative injury. Additionally, apoptotic RPE cell death was also induced by hydroquinone, a potent pro-oxidative component in cigarette tar<sup>11,12</sup>. Hydroquinone also suppresses the RPE expression of MCP1 and thereafter impedes the recruitment of scavenging macrophages, which ultimately accelerates the deposition of pro-inflammatory debris in the RPE<sup>13</sup>.

S-allyl L-cysteine (SAC), as the most abundant ingredient derived from fermented black garlic, exhibits a variety of beneficial functions including anti-carcinoma<sup>14,15</sup>, anti-oxidation<sup>16-20</sup>, anti-diabetes<sup>17,21</sup>, anti-inflammation<sup>17,21</sup>, and neuroprotection<sup>20,22</sup>. Overwhelming lines of evidence demonstrate that SAC effectively alleviates cell apoptosis induced by oxidative stress by promoting the antioxidant defense system<sup>16,23-26</sup>. However, the effect of SAC on hydroquinone exposure-related RPE apoptosis remains elusive. We herein evaluated the protective function of SAC in RPE impairments induced by hydroquinone and investigated the underlying mechanisms.

## Materials and Methods

### Cell Culture

Human retinal pigment epithelial cell line ARPE-19 was purchased from the Cell Bank of Type Culture Collection of Chinese Academy of Sciences (Shanghai, China) and grown in Dulbecco's Modified Eagle's Medium/F12 (DMEM/F12) medium (Gibco, Grand Island, NY, USA) containing 10% fetal bovine serum (FBS, Gibco, Grand Island, NY, USA) and 1% penicillin-streptomycin (Sigma-Aldrich, St Louis, MO, USA). The cells were maintained at 37°C in a humidified atmosphere of 5% CO<sub>2</sub> and starved overnight with the serum-free DMEM/F12 medium until growing to 80% confluence, before they were subjected to further experiments.

### Preparation of Agents

SAC (Sigma-Aldrich, St Louis, MO, USA) was diluted with phosphate-buffer solution (PBS) and stored at -20°C, with a stock concentration of 50 mM. Hydroquinone (Adamas, Shanghai, China) was freshly prepared for every experiment. It was dissolved in PBS and diluted to a final concentration of 200 µM.

### Cell Counting Kit-8 (CCK-8) Assay

RPE cell viability was assessed using the Cell Counting Kit-8 (MeilunBio, Dalian, Liaoning, China) according to the manufacturer's protocols. In brief, the cells (5×10<sup>3</sup> cells/well) were plated into 96-well plates and grown to 80% confluence. After being quiescent overnight with the serum-free DMEM/F12 medium, the cells were pre-treated with SAC for 2 h followed by incubation with 200 µM hydroquinone for 48 h. Afterward, 10 µL of CCK-8 solution was added to each well, and the cells were incubated at 37°C for other 2 h. The absorbance of the samples was measured at 450 nm using a microplate reader (Bio-Rad, Hercules, CA, USA).

### Terminal Deoxynucleotidyl Transferase-Mediated dUTP-Biotin Nick End Labeling (TUNEL) Assay

Apoptotic cells were detected using the *in situ* cell death detection kit (Roche Diagnostics, Mannheim, Germany) following the manufacturer's protocol. Briefly, the cells on the coverslips were fixed in 4% PFA for 25 min before permeabilization for 2 min on ice with 0.1% citrate buffer supplemented with 0.1% Triton X-100. Afterward, the coverslips were incubated at 37°C in TUNEL reaction mix containing nucleotides and terminal deoxynucleotidyl transferase (TdT) for 1 h. DAPI reagent was added after three washes with PBS, and the coverslips were mounted to a slide. TUNEL staining-positive cells were visualized under a fluorescence microscope (Olympus, Melville, NY, USA).

### Flow Cytometry

Annexin V-fluorescein isothiocyanate (FITC)/Propidium Iodide (PI) apoptosis detection kit (BD Biosciences, San Jose, CA, USA) was used to assess the apoptosis rate of ARPE19 cells. The cells were harvested and washed twice with pre-chilled PBS, and resuspended in binding buffer, and then incubated with 5 µL of annexin V-FITC and 5 µL of PI for 15 min in the dark before they were subjected to analysis with a flow cytometer (FACScan, BD Biosciences, San Jose, CA, USA).

### **Reactive Oxygen Species (ROS) Analysis**

The content of ROS in ARPE19 cells was measured using the specific ROS detection kit (MeilunBio, Dalian, China). In brief, the cells were pre-treated with 50  $\mu\text{M}$  SAC for 2 h and then incubated with 200  $\mu\text{M}$  hydroquinone for another 2 h, followed by the addition of 10  $\mu\text{M}$  DCFH-DA and 1 hour-incubation at 37°C in the dark. After washing thoroughly with serum-free medium, the cells were observed under an inverted fluorescence microscope. ROS production was determined by fluorescence spectroscopy with excitation/emission at 488 nm / 525 nm.

### **Morphological Examination**

The cells were seeded into 6-well plate and treated with 50  $\mu\text{M}$  SAC for 2 h at 80% confluence, followed by exposure to 200  $\mu\text{M}$  hydroquinone and incubation for 48 h. Cell morphological changes were observed under an inverted phase-contrast microscope (Olympus, Melville, NY, USA).

### **Western Blotting**

The total proteins were extracted from cell lysates with radioimmunoprecipitation assay (RIPA) lysis buffer (Beyotime Biotechnology, Shanghai, China) and separated by sodium dodecyl sulphate-polyacrylamide gel electrophoresis (SDS-PAGE; 10% acrylamide) before being transferred to polyvinylidene difluoride (PVDF) membranes (Millipore, Billerica, MA, USA), which were then blocked with 5% non-fat milk for at least 1 h and incubated overnight at 4°C with specific primary antibodies against HO-1, NQO-1, SOD1, SOD2 (Cell Signaling Technology, Beverly, MA, USA), Nrf2 (Abcam, Cambridge, UK), or anti-tubulin (OriGene Technologies, Rockville, MD, USA). After rinsing with Tris-Buffered Saline and Tween 20 (TBST), the membrane was then incubated for 1 h at room temperature with horseradish peroxidase (HRP)-conjugated goat anti-rabbit or goat anti-mouse IgG (CWBio, Beijing, China). After rinsing with TBST, the labeled proteins were visualized with enhanced chemiluminescence (ECL) substrates (Millipore, Billerica, MA, USA).

### **Statistical Analysis**

Data are presented as means  $\pm$  SD (standard deviation). All experiments were repeated 3 times independently. The differences between the two groups were analyzed using the Student's *t*-test. The comparison between multiple

groups was done using One-way ANOVA test followed by the post-hoc test (Least Significant Difference). All statistical analyses were carried out using the Statistical Product and Service Solutions (SPSS) 19.0 software (SPSS, Inc., Chicago, IL, USA). A value of  $p < 0.05$  was considered statistically significant.

## **Results**

### **SAC Reverses the Impaired Cell Viability Caused by Hydroquinone in a Dose-Dependent Manner**

Human ARPE19 cells were treated with 200  $\mu\text{M}$  hydroquinone before the CCK-8 assay was performed. As shown in Figure 1A, there was a remarkable decline in cell viability after treatment for at least 48 h. In order to evaluate the impact of SAC on cell viability, ARPE-19 cells were pre-treated with a concentration series of SAC before hydroquinone exposure. The effect of SAC on cell viability was barely detectable when it was employed alone (Figure 1B,  $p > 0.05$ ). Of note, the impaired cell viability caused by hydroquinone was reversed in the presence of SAC (Figure 1C,  $p < 0.05$ ), and this effect was quite evident when the concentration of SAC was only 2  $\mu\text{M}$ . The cell viability was increased in parallel with the elevation of SAC concentration and reached a peak value when it was increased to 50  $\mu\text{M}$ .

### **SAC Suppresses Hydroquinone-Induced RPE Cell Apoptosis**

ARPE-19 cells were exposed to hydroquinone with or without pretreatment of SAC, after which the cells were examined for apoptotic status by using flow cytometry and TUNEL assay. According to the Annexin-V/PI flow cytometry analysis (Figure 2A), the proportion of apoptotic cells was dramatically elevated upon hydroquinone stimulation in the absence of SAC ( $p < 0.05$ ). The results also showed that the cell apoptosis rate was significantly hindered when ARPE-19 cells were treated with hydroquinone in combination with SAC. Likewise, under the fluorescence microscopy, we observed that SAC addition resulted in a decrease in fluorescein-labeled apoptotic cells when compared to the cells treated with hydroquinone alone (Figure 2B,  $p < 0.05$ ). These data indicate that pre-exposure to SAC mitigates hydroquinone induced RPE cell apoptosis while SAC *per se* has no effect on these cells.

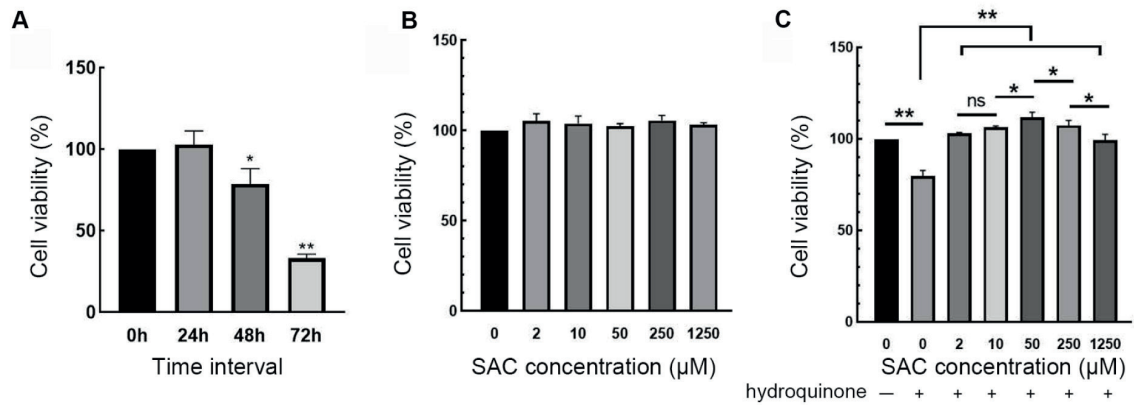


**Figure 1.** SAC protects RPE cells from hydroquinone-induced death. **A**, ARPE-19 cells were stimulated with 200 μM hydroquinone and cell viability was evaluated at different time intervals by using CCK-8 assay. \* $p < 0.05$ ; \*\* $p < 0.01$  compared with the control group.  $n = 3$  independent experiments. **B**, The cells were treated with SAC of escalating concentrations for 48 h, followed by assessment of cell viability. **C**, The cells were pre-treated with SAC for 2 h, and then incubated with 200 μM hydroquinone for another 48 h. \* $p < 0.05$ ; \*\* $p < 0.01$ ; and ns indicated that the difference is not significant.  $n = 3$  independent experiments.

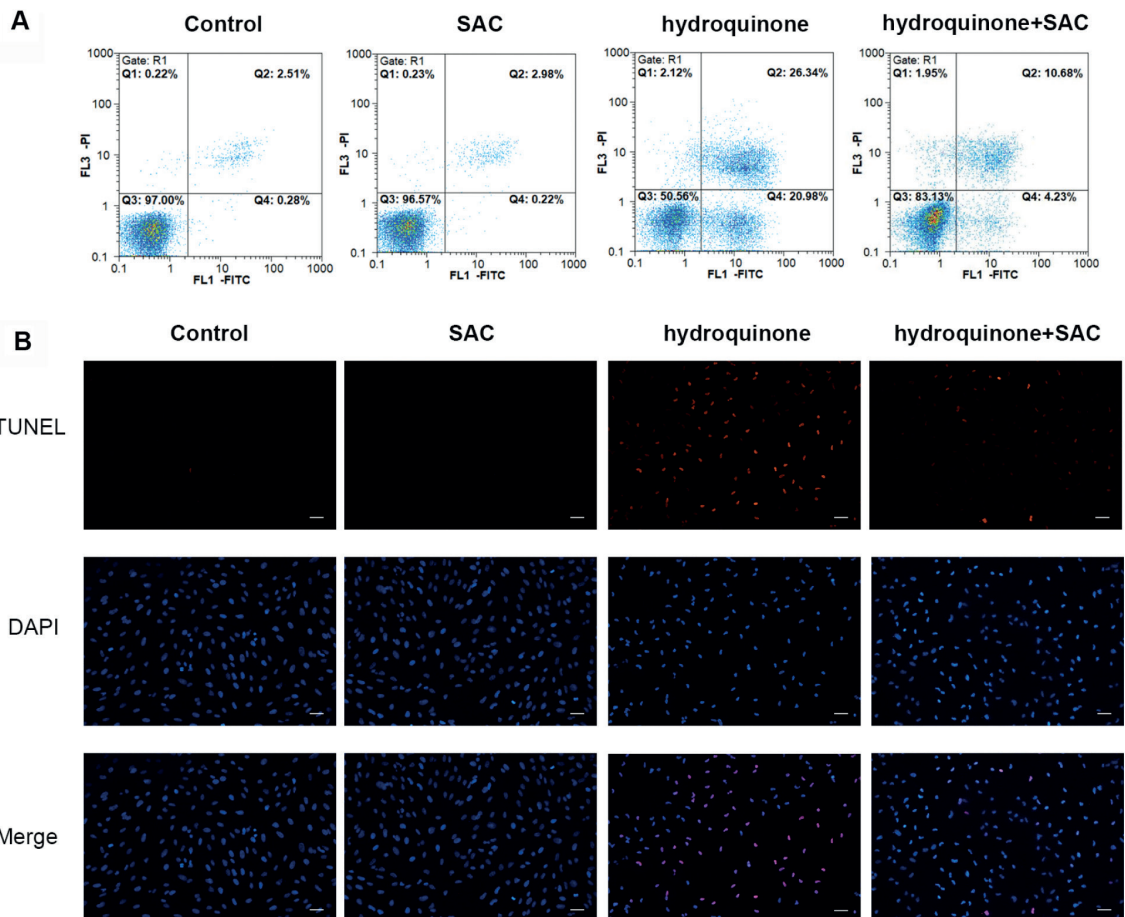


**Figure 2.** Hydroquinone induces apoptosis in ARPE-19 cells, which was attenuated by SAC. ARPE-19 cells were exposed to 200 μM hydroquinone for 24 h in the presence or absence of 2 h-pretreatment of 50 μM SAC. The apoptosis rate of ARPE-19 cells was detected by flow cytometric analysis (**A**) or TUNEL assay (**B**, scale bar: 100 μm). \*\* $p < 0.01$  compared to the control group; and ## $p < 0.01$  compared with cells treated with hydroquinone alone. **C**, Representative images of the morphological changes of ARPE-19 cells in different groups (scale bar: 100 μm).

Figure continued

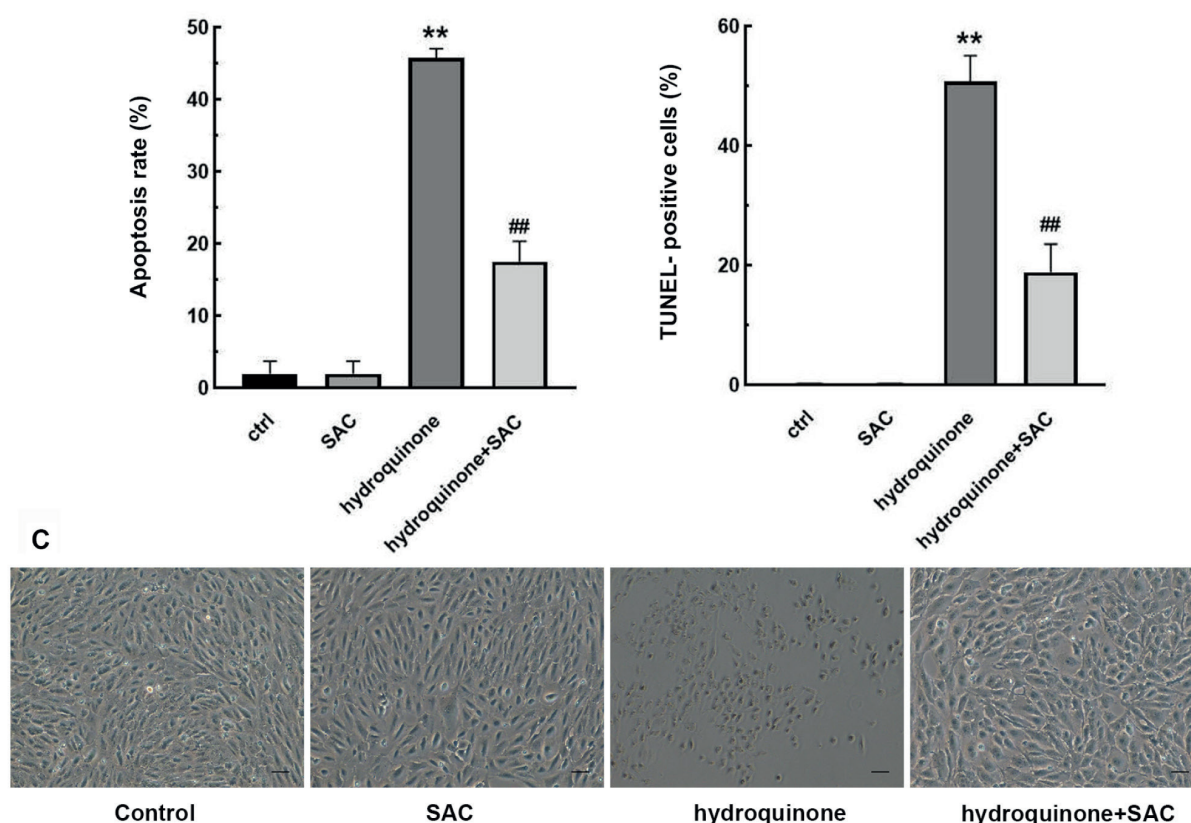


**Figure 2.** (Continued). Hydroquinone induces apoptosis in ARPE-19 cells, which was attenuated by SAC. ARPE-19 cells were exposed to 200  $\mu$ M hydroquinone for 24 h in the presence or absence of 2 h- pretreatment of 50  $\mu$ M SAC. The apoptosis rate of ARPE-19 cells was detected by flow cytometric analysis (A) or TUNEL assay (B, scale bar: 100  $\mu$ m). \*\* $p$ <0.01 compared to the control group; and ## $p$ <0.01 compared with cells treated with hydroquinone alone. C, Representative images of the morphological changes of ARPE-19 cells in different groups (scale bar: 100  $\mu$ m).

### **SAC Attenuates the Morphological Changes of ARPE-19 Cells Treated With Hydroquinone**

In addition, to verify the inhibitory effect of SAC on hydroquinone-induced cell apoptosis, morphological changes in ARPE-19 cells were observed under an inverted microscope. As shown in Figure 2C, normal RPE cells were in a typical spindle-shaped and elongated shape. Also, SAC exposure did not lead to apparent morphological changes in RPE cells. Following hydroquinone exposure, the number of adherent cells decreased, and the cells displayed characteristic apoptotic morphology, including cell shrinkage, chromatin condensation, and the formation of apoptosis body-like structures. However, the abovementioned apoptotic phenotype was not found in the hydroquinone-treated cells undergoing pretreatment with SAC.

### **SAC Decreases ROS Generation Induced by Hydroquinone**

To determine whether hydroquinone-induced apoptosis is related to intracellular oxidative stress, the reactive oxygen species (ROS) level produced by ARPE-19 cells was assessed after hydroquinone treatment, in the presence or absence of SAC pretreatment. As shown in Figure 3A and 3B, hydroquinone stimulation contributed to a considerable increase in ROS generation in ARPE-19 cells ( $p$ <0.05), while the ROS production was not significantly altered in response to SAC treatment alone. Remarkably, after SAC pretreatment, the ROS level in hydroquinone-stimulated cells was evidently lower in comparison to the cells treated by hydroquinone alone ( $p$ <0.05). The results suggest that SAC probably protects ARPE-19 cells from oxidative-initiated apoptosis mainly by reducing ROS accumulation.

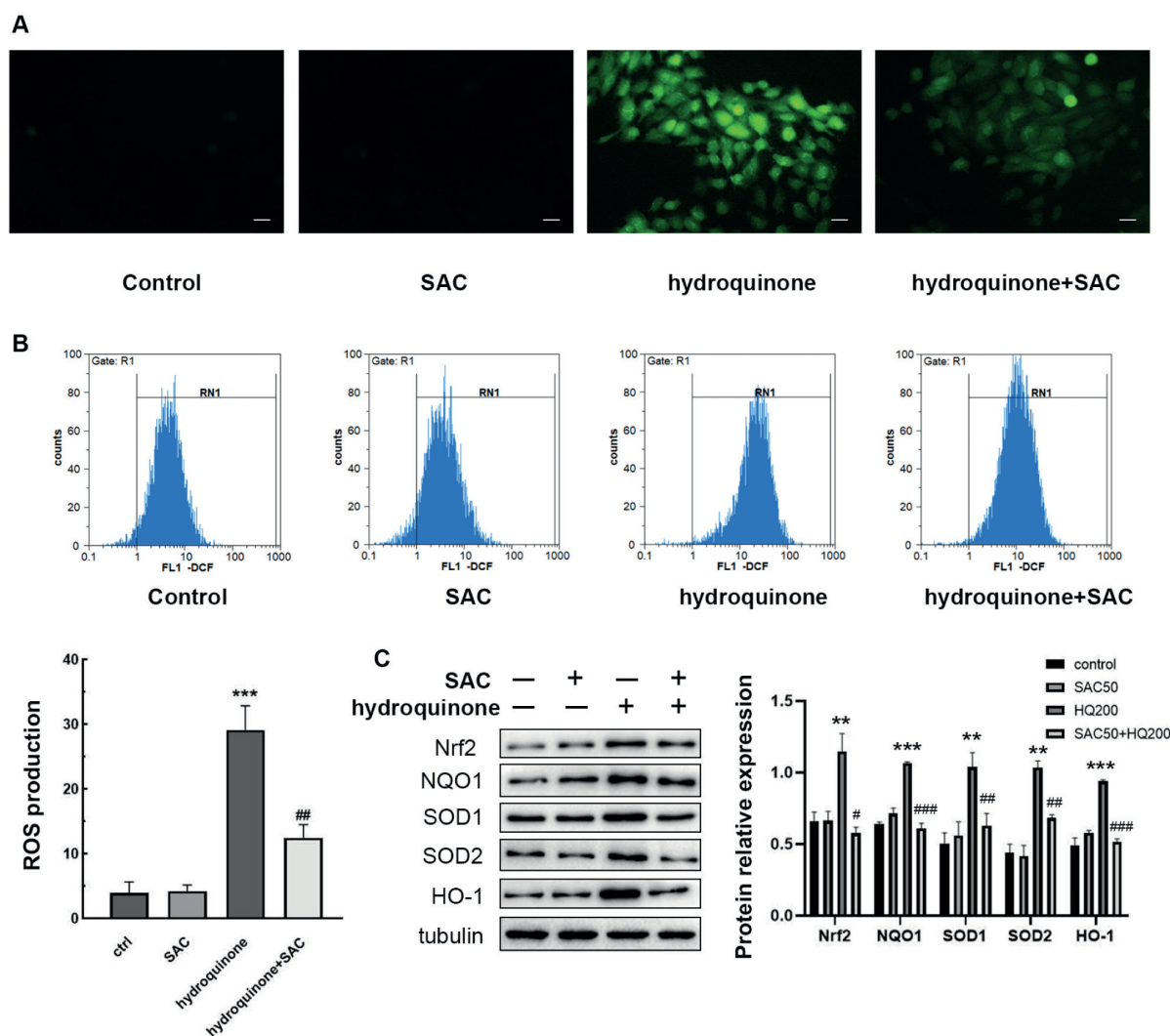


**Figure 3.** SAC mitigates hydroquinone-stimulated anti-oxidative response in RPE cells. ARPE-19 cells were exposed to 200  $\mu$ M hydroquinone in the presence or absence of pretreatment with 50  $\mu$ M SAC, and then (A) DCFH-DA-stained cells were observed under fluorescence microscope. Scale bar: 50  $\mu$ m. B, ROS production was otherwise assessed by flow cytometry with excitation/emission at 488 nm/525 nm. \*\*\* $p$ <0.001 compared to the control group; ## $p$ <0.01 compared with cells treated with hydroquinone alone. C, The expression levels of antioxidant-related proteins were measured by Western blot analysis. Tubulin was used as an internal control. \* $p$ <0.05, \*\* $p$ <0.01, \*\*\* $p$ <0.001 compared to the control group, and # $p$ <0.05, ## $p$ <0.01, and ### $p$ <0.001 compared with cells treated with hydroquinone alone.  $n$ =3 independent experiments.

### The Altered Expression Profiling of Anti-Oxidative Factors

Nrf2 is a key regulator of the cellular redox state and its activation promotes the transcription of several antioxidant mediators. As expected, treatment with low-dose SAC (50  $\mu$ M) did not lead to significant alterations in the expression of Nrf2 compared to the control group ( $p$ >0.05, shown in Figure 3C). Otherwise, Nrf2 expression in ARPE-19 cells was significantly aggrandized after hydroquinone incitement ( $p$ <0.01), because the cellular antioxidant defense was induced in

response to the oxidant hydroquinone. Also, the expression patterns of other antioxidant factors, including NQO1, SOD1, SOD2, and HO1 were examined through immunoblotting, where analogous results were observed. As shown in Figure 3B, SAC treatment did not change the expression of these proteins in ARPE-19 cells whereas their levels were evidently elevated after exposure to hydroquinone.

In parallel with SAC addition, intriguingly, the hydroquinone-induced augmented expression levels of the abovementioned antioxidant proteins

were remarkably decreased in comparison with those incited with hydroquinone alone, indicating that SAC effectively reduces the cellular oxidative stress irritated by hydroquinone.

## Discussion

So far, no effective therapeutic strategy has been developed for dry AMD, which ultimately progresses into irreversible visual impairments or loss. One of the principal pathological hallmarks of late-stage dry (atrophic) AMD is the malfunction and cell death of RPE<sup>4</sup>. Hydroquinone is a potent pro-oxidative component in cigarette smoke and it has been proposed to induce mitochondrion-mediated apoptotic RPE cell death<sup>5,27</sup>. Mitochondria are the primary source of cellular ATP and ROS production and, in addition, they contain a self-destructive arsenal of apoptotic factors that can be unleashed to promote cell apoptosis. As mentioned in previous study<sup>5</sup>, cigarette smoke exposure increased the mitochondrial ROS accumulation, which disturbed intracellular oxidative homeostasis and reduced mitochondrial potential, thereby causing mitochondria fragmented and diffusely distributed in RPE cells and ultimately contributing to cell apoptosis. On the other hand, hydroquinone can also suppress RPE expression of MCP1, a potent chemokine to recruit scavenging immunocytes, such as macrophages, and thereby exacerbate the accumulation of inflammatory debris in RPE, which contributes to the degenerative damage of it<sup>13</sup>. Therefore, we used human RPE cells treated with hydroquinone in the present work to mimic the oxidative damage which plays a significant role in AMD development<sup>28-31</sup>, and found that the viability of hydroquinone stimulated ARPE19 cells was significantly decreased (20.23% reduction from the control), whereas the apoptosis rate was higher than untreated cells ( $43.79\% \pm 1.04\%$  vs.  $2\% \pm 0.52\%$ ,  $p < 0.05$ ), and this was consistent with previous reports.

The antioxidant garlic derivative SAC was previously proved to exert neuroprotective effects on the kainite excitotoxicity-induced degenerative damage of retinal ganglion cells (RGCs), and thus prevent retinal ischemia which is responsible for the development of many ocular disorders<sup>22</sup>. Our results showed that pretreatment of SAC before the hydroquinone exposure resulted in a significant increase in RPE cell viability, and meanwhile, blunted the hydroquinone-induced cell apoptosis, as compared to those treated with hydroquinone

alone. The cell viability reached a peak value when SAC concentration was increased to 50  $\mu\text{M}$ , indicating that SAC exerts its protective effect on RPE cells even at a low concentration.

Envisioned as a sort of crucial signaling molecules, ROS participate in diverse physiological cell events, such as adaptation to hypoxia, autophagy, immunity, and differentiation<sup>32</sup>. However, redundant ROS may contribute to cell death through oxidation of membrane lipids and proteins, which is a fundamental pathomechanism of several oxidative stress-related diseases, such as diabetes mellitus and neurodegenerative diseases<sup>33</sup>. In the present study, the generation of ROS was found evidently aggrandized in ARPE19 cells treated with hydroquinone, in comparison to the untreated cells. In the presence of SAC, the augmented ROS production induced by hydroquinone was evidently abated, although treatment of SAC alone did not lead to significant changes in ROS level. These results suggest that SAC inhibits the hydroquinone-induced apoptosis of ARPE19 cells by, at least in part, impinging on the oxidation-related signaling pathways.

In this context, an essential antioxidant mediator Nrf2 was dramatically upregulated after ARPE19 cells were treated with hydroquinone, which reflected increased oxidative stress upon hydroquinone stimulation. This agrees with previous study displaying that Nrf2 acts as a response factor to reduce oxidative stress and protect RPE cells from cigarette smoke-induced apoptosis<sup>27,34-36</sup>. Notably, when ARPE19 cells were pre-treated with SAC before hydroquinone stimulation, the enhanced expression of Nrf2 induced by hydroquinone was significantly suppressed. Furthermore, similar changes were observed in the expression of downstream antioxidant genes, including NQO1, SOD1, SOD2, and HO1. These data suggest that SAC protects ARPE-19 cells from apoptosis mainly by repressing hydroquinone-triggered oxidative stress.

To the best of our knowledge, it is the first time that SAC has been proved to alleviate the hydroquinone-initiated oxidative damage within human RPE cells, which is tightly related to AMD pathogenesis<sup>37-39</sup>, thereafter driving the improvement of novel therapeutic strategies. However, our *in vitro* data are not adequate to conclude that SAC can directly ameliorate the development of AMD. The rats exposed to additional oxidative stresses, such as sodium iodate and cigarette smoke/hydroquinone, usually serve as representative animal models for AMD

and they have helped to reveal the underlying pathological mechanisms of this disease. These animal models are applied in our on-going experiments to verify the protective role of SAC in the development of AMD, and further results will be published in the future.

## Conclusions

In summary, our results demonstrate that SAC effectively attenuates hydroquinone-induced oxidative damage in human RPE cells, represented by the significantly reduced apoptosis and ROS production. Furthermore, the pretreatment of SAC downregulated Nrf2, which was induced otherwise by hydroquinone, and similar alterations of expression profiles were observed in the downstream antioxidant genes. These data suggest that SAC exerts its effects by suppressing cell response to the detrimental oxidative stress initiated by hydroquinone.

## Conflict of Interests

The Authors declare that they have no conflict of interests.

## Acknowledgments

The authors wish to thank Dr Zhulin Hu and Dr Chen Chen for their experimental design and technology help. This work was financially supported by the National Natural Science Foundation of China (NSFC, Grant Number 81660167); the Science and Technology Project of Yunnan Province (Grant Number 2017FB114); Key Laboratory of Yunnan Province for the Prevention and Treatment of Ophthalmology (2017DG008); Technical Research for the Prevention and Treatment of Important Ocular Surface Diseases (2018ZF009); Provincial Innovation Team for Cataract and Ocular Fundus Disease, The Second People's Hospital of Yunnan Province (2017HC010); and Expert Workstation of Yao Ke (2017IC064) and Graduate Innovation Fund of Kunming Medical University (2019S197).

## References

- 1) CHOU R, DANA T, BOUGATSOS C, GRUSING S, BLAZINA I. Screening for impaired visual acuity in older adults: updated evidence report and systematic review for the US preventive services task force. *JAMA* 2016; 315: 915-933.
- 2) HAJAR S, AL HA, WASLI M, MOUSA A, RABIU M. Prevalence and causes of blindness and diabetic retinopathy in Southern Saudi Arabia. *Saudi Med J* 2015; 36: 449-455.
- 3) YANG Y, WU ZZ, CHENG YL, LIN W, QU C. Resveratrol protects against oxidative damage of retinal pigment epithelium cells by modulating SOD/MDA activity and activating Bcl-2 expression. *Eur Rev Med Pharmacol Sci* 2019; 23: 378-388.
- 4) TOTSUKA K, UETA T, UCHIDA T, ROGGIA MF, NAKAGAWA S, VAVVAS DG, HONJO M, AIHARA M. Oxidative stress induces ferroptotic cell death in retinal pigment epithelial cells. *Exp Eye Res* 2019; 181: 316-324.
- 5) CHEN C, CANO M, WANG JJ, LI J, HUANG C, YU Q, HERBERT TP, HANDA JT, ZHANG SX. Role of unfolded protein response dysregulation in oxidative injury of retinal pigment epithelial cells. *Antioxid Redox Signal* 2014; 20: 2091-2106.
- 6) FERRIS FL, DAVIS MD, CLEMONS TE, LEE LY, CHEW EY, LINDBLAD AS, MILTON RC, BRESSLER SB, KLEIN R; Age-Related Eye Disease Study (AREDS) Research Group. A simplified severity scale for age-related macular degeneration: AREDS Report No. 18. *Arch Ophthalmol* 2005; 123: 1570-1574.
- 7) KIJLSTRA A, BERENDSCHOT TT. Age-related macular degeneration: a complementopathy? *Ophthalmic Res* 2015; 54: 64-73.
- 8) PONS M, MARIN-CASTAÑO ME. Nicotine increases the VEGF/PEDF ratio in retinal pigment epithelium: a possible mechanism for CNV in passive smokers with AMD. *Invest Ophthalmol Vis Sci* 2011; 52: 3842-3853.
- 9) WOO SJ, AHN J, MORRISON MA, AHN SY, LEE J, KIM KW, DEANGELIS MM, PARK KH. Analysis of genetic and environmental risk factors and their interactions in Korean patients with age-related macular degeneration. *PLoS One* 2015; 10: e0132771.
- 10) FUJIHARA M, NAGAI N, SUSSAN TE, BISWAL S, HANDA JT. Chronic cigarette smoke causes oxidative damage and apoptosis to retinal pigmented epithelial cells in mice. *PLoS One* 2008; 3: e3119.
- 11) TSUJINAKA H, ITAYA-HIRONAKA A, YAMAUCHI A, SAKURAMOTO-TSUCHIDA S, OTA H, TAKEDA M, FUJIMURA T, TAKASAWA S, OGATA N. Human retinal pigment epithelial cell proliferation by the combined stimulation of hydroquinone and advanced glycation end-products via up-regulation of VEGF gene. *Biochem Biophys Rep* 2015; 2: 123-131.
- 12) LIU J, YUAN Q, LING X, TAN Q, LIANG H, CHEN J, LIN L, XIAO Y, CHEN W, LIU L, TANG H. PARP1 may be involved in hydroquinone-induced apoptosis by poly ADP-ribosylation of ZO-2. *Mol Med Rep* 2017; 16: 8076-8084.
- 13) PONS M, MARIN-CASTAÑO ME. Cigarette smoke-related hydroquinone dysregulates MCP-1, VEGF and PEDF expression in retinal pigment epithelium in vitro and in vivo. *PLoS One* 2011; 6: e16722.
- 14) PAI MH, KUO YH, CHIANG EP, TANG FY. S-Allylcysteine inhibits tumour progression and the epithelial-mesenchymal transition in a mouse xenograft model of oral cancer. *Br J Nutr* 2012; 108: 28-38.
- 15) XU YS, FENG JG, ZHANG D, ZHANG B, LUO M, SU D, LIN NM. S-allylcysteine, a garlic derivative, suppresses proliferation and induces apoptosis in human ovarian cancer cells in vitro. *Acta Pharmacol Sin* 2014; 35: 267-274.



- 16) KATTAIA AA, ABD ES, MOHAMED EM, ABDUL-MAKSOU RS, ELFAKHARANY YM. Molecular mechanisms underlying histological and biochemical changes induced by nitrate in rat liver and the efficacy of S-allylcysteine. *Ultrastruct Pathol* 2017; 41: 10-22.
- 17) BALUCHNEJADMOJARAD T, KIASALARI Z, AFSHIN-MAJD S, GHASEMI Z, ROGHANI M. S-allyl cysteine ameliorates cognitive deficits in streptozotocin-diabetic rats via suppression of oxidative stress, inflammation, and acetylcholinesterase. *Eur J Pharmacol* 2017; 794: 69-76.
- 18) FRANCO-ENZASTIGA U, SANTANA-MARTINEZ RA, SILVA-ISLAS CA, BARRERA-OVIEDO D, CHANEZ-CARDENAS ME, MALDONADO PD. Correction to: chronic administration of S-allylcysteine activates Nrf2 factor and enhances the activity of antioxidant enzymes in the striatum, frontal cortex and hippocampus. *Neurochem Res* 2018; 43: 513-514.
- 19) OROZCO-IBARRA M, MUÑOZ-SÁNCHEZ J, ZAVALA-MEDINA ME, PINEDA B, MAGAÑA-MALDONADO R, VÁZQUEZ-CONTRERAS E, MALDONADO PD, PEDRAZA-CHAVERRI J, CHÁNEZ-CÁRDENAS ME. Aged garlic extract and S-allylcysteine prevent apoptotic cell death in a chemical hypoxia model. *Biol Res* 2016; 49: 7.
- 20) ROJAS P, SERRANO-GARCÍA N, MEDINA-CAMPOS ON, PEDRAZA-CHAVERRI J, MALDONADO PD, RUIZ-SÁNCHEZ E. S-Allylcysteine, a garlic compound, protects against oxidative stress in 1-methyl-4-phenylpyridinium-induced parkinsonism in mice. *J Nutr Biochem* 2011; 22: 937-944.
- 21) SATHIBABU UDDANDRAO VV, BRAHMANAIDU P, RAVINDARNAIK R, SURESH P, VADIVUKKARASI S, SARAVANAN G. Restorative potentiality of S-allylcysteine against diabetic nephropathy through attenuation of oxidative stress and inflammation in streptozotocin-nicotinamide-induced diabetic rats. *Eur J Nutr* 2019; 58: 2425-2437.
- 22) CHAO HM, CHEN IL, LIU JH. S-allyl L-cysteine protects the retina against kainate excitotoxicity in the rat. *Am J Chin Med* 2014; 42: 693-708.
- 23) KALAYARASAN S, SRIRAM N, SURESHKUMAR A, SUDHANDIRAN G. Chromium (VI)-induced oxidative stress and apoptosis is reduced by garlic and its derivative S-allylcysteine through the activation of Nrf2 in the hepatocytes of Wistar rats. *J Appl Toxicol* 2008; 28: 908-919.
- 24) PADIYA R, CHOWDHURY D, BORKAR R, SRINIVAS R, PAL BM, BANERJEE SK. Garlic attenuates cardiac oxidative stress via activation of PI3K/AKT/Nrf2-Keap1 pathway in fructose-fed diabetic rat. *PLoS One* 2014; 9: e94228.
- 25) QU Z, MENG F, BOMGARDEN RD, VINER RI, LI J, ROGERS JC, CHENG J, GREENLIEF CM, CUI J, LUBAHN DB, SUN GY, GU Z. Proteomic quantification and site-mapping of S-nitrosylated proteins using isobaric iodoTMT reagents. *J Proteome Res* 2014; 13: 3200-3211.
- 26) CRUZ C, CORREA-ROTTER R, SANCHEZ-GONZALEZ DJ, HERNANDEZ-PANDO R, MALDONADO PD, MARTINEZ-MARTINEZ CM, MEDINA-CAMPOS ON, TAPIA E, AGUILAR D, CHIRINO YI, PEDRAZA-CHAVERRI J. Renoprotective and antihypertensive effects of S-allylcysteine in 5/6 nephrectomized rats. *Am J Physiol Renal Physiol* 2007; 293: F1691-F1698.
- 27) HUANG C, WANG JJ, MA JH, JIN C, YU Q, ZHANG SX. Activation of the UPR protects against cigarette smoke-induced RPE apoptosis through up-regulation of Nrf2. *J Biol Chem* 2015; 290: 5367-5380.
- 28) BEATTY S, KOH H, PHIL M, HENSON D, BOULTON M. The role of oxidative stress in the pathogenesis of age-related macular degeneration. *Surv Ophthalmol* 2000; 45: 115-134.
- 29) YILDIRIM Z, UCGUN NI, YILDIRIM F. The role of oxidative stress and antioxidants in the pathogenesis of age-related macular degeneration. *Clinics (Sao Paulo)* 2011; 66: 743-746.
- 30) SHAW PX, STILES T, DOUGLAS C, HO D, FAN W, DU H, XIAO X. Oxidative stress, innate immunity, and age-related macular degeneration. *AIMS Mol Sci* 2016; 3: 196-221.
- 31) DANULESCU R, COSTIN D. The assessment of treatment efficacy in age related macular degeneration by evaluating the oxidative stress markers and OCT measurements. *Rev Med Chir Soc Med Nat Iasi* 2013; 117: 328-333.
- 32) SENA LA, CHANDEL NS. Physiological roles of mitochondrial reactive oxygen species. *Mol Cell* 2012; 48: 158-167.
- 33) NITA M, GRZYBOWSKI A. The role of the reactive oxygen species and oxidative stress in the pathomechanism of the age-related ocular diseases and other pathologies of the anterior and posterior eye segments in adults. *Oxid Med Cell Longev* 2016; 2016: 3164734.
- 34) TELKOPARAN-AKILLILAR P, SUZEN S, SASO L. Pharmacological applications of Nrf2 inhibitors as potential antineoplastic drugs. *Int J Mol Sci* 2019; 20: pii: 2025.
- 35) SIVANDZADE F, BHALERAO A, CUCULLO L. Cerebrovascular and neurological disorders: protective role of NRF2. *Int J Mol Sci* 2019; 20: pii: E3433.
- 36) LIU C, WU QQ, CAI ZL, XIE SY, DUAN MX, XIE QW, YUAN Y, DENG W, TANG QZ. Zingerone attenuates aortic banding-induced cardiac remodelling via activating the eNOS/Nrf2 pathway. *J Cell Mol Med* 2019; 23: 6466-6478.
- 37) MUANGNOI C, SHARIF U, RATNATILAKA NBP, ROJSITTHISAK P, PARAOAN L. Protective effects of curcumin ester prodrug, curcumin diethyl disuccinate against H2O2-induced oxidative stress in human retinal pigment epithelial cells: potential therapeutic avenues for age-related macular degeneration. *Int J Mol Sci* 2019; 20: pii: E3367.
- 38) HUANG SY, CHANG SF, CHAU SF, CHIU SC. The protective effect of Hispidin against hydrogen peroxide-induced oxidative stress in ARPE-19 cells via Nrf2 signaling pathway. *Biomolecules* 2019; 9: pii: 380.
- 39) TOHARI AM, ALHASANI RH, BISWAS L, PATNAIK SR, REILLY J, ZENG Z, SHU X. Vitamin D attenuates oxidative damage and inflammation in retinal pigment epithelial cells. *Antioxidants (Basel)* 2019; 8: pii: E341.